HHS Public Access

Author manuscript

J Am Chem Soc. Author manuscript; available in PMC 2016 November 15.

Published in final edited form as:

J Am Chem Soc. 2016 July 27; 138(29): 9073–9076. doi:10.1021/jacs.6b05428.

Modular Artificial Cupredoxins

Samuel I. Mann[§], **Tillmann Heinisch**[¶], **Andrew C. Weitz**[†], **Michael P. Hendrich**[†], **Thomas R. Ward**[¶], and **A. S. Borovik**[§,*]

[§]Department of Chemistry, University of California-Irvine, 1102 Natural Sciences II, Irvine, CA 92697 [¶]Department of Chemistry, University of Basel, Spitalstrasse 51, CH-4056 Basel, Switzerland [†]Department of Chemistry, Carnegie Mellon University, Pittsburgh, PA 15213

Abstract

Cupredoxins are electron transfer proteins that have active sites containing a monomeric Cu center with an unusual trigonal monopyramidal structure (Type 1 Cu). A single Cu-S_{cys} bond is present within the trigonal plane that is responsible for its unique physical properties. We demonstrate that a cysteine-containing variant of streptavidin (Sav) can serve as a protein host to model the structure and properties of Type 1 Cu sites. A series of artificial Cu proteins are described that rely on Sav and a series of biotinylated synthetic Cu complexes. Optical and EPR measurements highlight the presence of a Cu–S_{cys} bond and XRD analysis provide structural evidence. We further provide evidence that changes in the linker between the biotin and Cu complex within the synthetic constructs allows for small changes in the placement of Cu centers within Sav that have dramatic effects on the structural and physical properties of the resulting artificial metalloproteins. These findings highlight the utility of the biotin-Sav technology as an approach for simulating active sites of metalloproteins.

Metalloproteins perform a wide range of chemical transformations whose functions have yet to be achieved by artificial systems. The discrepancy in reactivity can be directly linked to the inability of most unnatural systems to duplicate the precise structural control of the primary and secondary coordination spheres that are present within the active sites of proteins. Numerous synthetic systems and artificial metallo-protein (ArMs) have been developed to regulate both coordination spheres and notable successes have been achieved.[1-9] Biotin-streptavidin (Sav) technology has been found to be an effective method for placing metal complexes in specific locations within a protein thanks to Sav's unusually high affinity for biotin ($K_b > 10^{14}$ M^{-1}).[10] For instance, ArMs comprised of biotinylated organometallic complexes and Sav catalyze a variety of organic transformations, many of which having impressive selectivities.[11,12] We have extended this approach toward developing artificial Cu-proteins whose primary and secondary coordination sphere can be

Correspondence to: Michael P. Hendrich; Thomas R. Ward.

[*]**Corresponding Author** aborovik@uci.edu.

ASSOCIATED CONTENT

Experimental details for all reactions, physical and XRD measurements, Figures S1-S8, and electron density overlays for all protein structures. This material is available free of charge via the Internet at http://pubs.acs.org.

systematically modulated. We show herein that biotinylated Cu complexes can be confined within Sav to prepare ArMs that have properties similar to those of cupredoxins.

Cupredoxins have a central role in biological electron transfer processes and contain active sites with a single copper center (referred to as Type I Cu centers, Figure 1A) with unusual structural and spectroscopic properties, and relatively high redox potentials (180-800 mV vs NHE).[3,13] Detailed structure-function studies have found that "classic" Type 1 centers, such as that in *Alcaligenes denitrificans* azurin, have Cu sites with unique coordination geometries that are best characterized as distorted trigonal monopyramidal. The trigonal plane contains two N-atom donors from histidine residues and one S-atom donor from a cysteine thiolate; the axial ligand can vary but is often an S-atom from a methionine thioether that only weakly interacts with the Cu center ($Cu–S_{met} > 2.8$ Å). The highly covalent Cu(II)–S(thiolate) bond is responsible for the distinct color that arises from an intense S_{π}–Cu ligand-to-metal charge transfer (LMCT) band at $\lambda_{max} \sim 600$ nm (ε_M = 3000-6000), as well as the small Cu hyperfine coupling of $A_z \sim 180$ MHz. Variations within cupredoxins exist that are manifested in different structural and spectroscopic properties. These "perturbed" sites (e.g., *Rhus vernicifera* stellacyanin) have an absorbance band at $\lambda_{max} \sim 600$ nm but exhibit an additional feature at $\lambda_{max} \sim 450$ nm.[14,15] Solomon has defined the parameter $R\varepsilon = \varepsilon_{450}/\varepsilon_{600}$ to distinguish between the various Type 1 Cu sites: an $R\varepsilon$ of less than 0.15 is considered a classical site whereas those with larger values are perturbed sites.[13] In addition to their unique primary coordination spheres, the secondary coordination spheres about the Cu centers in cupredoxins impact function. These effects are elegantly illustrated in the work of Lu who used mutagenesis methods to re-engineer the active site in azurin to vary the reduction potential by nearly 2 V.[9]

It has been a challenge to reproduce the structural, spectroscopic, and redox properties of Type 1 Cu sites within artificial systems. Attempts to model these active sites include metallopeptides with sequences that contain the loop of cupredoxins[16] and three-helix bundles[17] that assemble to form a Type 1 Cu binding site. In addition, synthetic Cu complexes have been prepared with sterically constrained ligands that have been useful in investigating the details of the Cu^{II}–S(thiolate) interaction.[18-20] However, there are few synthetic examples that can simulate the properties of Type 1 Cu sites, but none that incorporates a biologically relevant S-donor from cysteine.

We selected the biotinylated di[2-(2-pyridyl)ethyl]amine (dpea), which is a tridentate ligand that Karlin has shown to tightly bind to Cu^{II} ions.[21] Three constructs were prepared that differed by the linker group between the biotin and dpea (biot-R-dpea, where R = et, pr, bu) via a 3-step route from dpea (Scheme S1). Formation of the Cu^{II} complexes was achieved by treating biot-R-dpea with $CuCl_2$ in CH_3CN to afford $[Cu^{II}(\text{biot-R-dpea})(Cl)(H_2O)]Cl$. The ArMs $[Cu^{II}(\text{biot-R-dpea})(H_2O)_2]^{2+} \subset$ Sav WT (R = et (**1a**); pr (**1b**); bu (**1c**)) were prepared by incubating Sav WT at pH 6 in MES buffer (50 mM) with a DMF solution of $[Cu^{II}(\text{biot-R-dpea})(Cl)(H_2O)]Cl$ for 5 min. A 4:1 ratio of each $[Cu^{II}(\text{biot-R-dpea})(Cl)(H_2O)]Cl$ complex to Sav WT was determined using the (2-(4′-hydroxyazo-benzene)benzoic acid assay[22] (Figure S1), indicating that each subunit contains one Cu complex. The spectroscopic properties support the formation of the artificial Cu proteins; protein solutions have weak bands at $\lambda_{max} \sim 650$ ($\varepsilon_M \sim 50$) that are assigned to d-d transitions for the

immobilized Cu(II) centers (Figures 2 & S2A, Table S1). The EPR spectra for **1a-c** are nearly identical and were simulated for species with S = 1/2 spin ground states. In addition, each spectrum contained two sets of signals of equal intensity (Figure S3) that we suggest are caused by the immobilized Cu(II) complex adopting two orientations (Table S1).

Single crystals of **1a** were prepared by soaking crystals of apo-Sav WT with $[Cu^{II}$(biot-et-dpea)$(H_2O)_2]^{2+}$. Its structure was solved to 1.72 Å resolution[23] to reveal a single Cu(II) complex housed within each subunit of Sav WT arranged in a trigonal bipyramidal geometry, in which the primary coordination sphere is composed of 3 nitrogen atoms from the dpea ligand and 2 oxygen donors from aquo ligands (Figure S4A, Table S2). The dpea ligand binds in a meridional fashion to the copper center with an average Cu–N bond length of 1.98 (1) Å.[24] Note that O1 is also part of an H-bonding network that includes S112, the carbonyl of A86, and a structural water molecule.

The structural results for **1a** indicate that targeting position 112 may offer a suitable site to install an endogenous donor that could bind to the immobilized Cu complex. Previous work has shown that the imidazole residue in the $S_{112}H$ variant can coordinate to and immobilize a biotinylated Rh complex.[25] Rather than using $S_{112}H$ as the host, we prepared new artificial Cu proteins using $S_{112}C$ variant with the goal to design ArMs with Cu sites that are similar to those found in cupredoxins. The confinement of complexes within a subunit should prevent intermolecular interactions that often hinder the formation of discrete $Cu–S_{cys}$ complexes in synthetic systems. For instance, reactions with free $[Cu^{II}$(biot-pr-dpea)$(H_2O)Cl]Cl$ complex and various thiols including the cysteine derivative *N*-(*tert*-butoxycarbonyl)-L-cysteine methyl ester in DMF, led to a loss of the Cu^{II} complex presumably through reduction and formation of disulfide species (Figure S5). To form discrete and stable complexes with $Cu–S_{cys}$ bonds, the $S_{112}C$ variant was incubated with $[Cu^{II}$(biot-R-dpea)$(Cl)(H_2O)]Cl$ using the conditions described above for Sav WT to produce $[Cu^{II}$(biot-R-dpea)$S_{cys112}^{+} \subset$ Sav $S_{112}C$ (R = et, (**2a**), pr, (**2b**), bu, (**2c**)).

ArM **2a** exhibited optical features that were significantly different from those of **1** with an electronic absorption spectrum containing intense bands at λ_{max} (ε_M) = 445 (1020), 570 (1010), and 770 (700) (Figure 2, Table 2). These data produced an $R\varepsilon$ = 0.95, which is similar to the value of 0.82 reported for the purple cupredoxin Nmar1307.[29] Structural information obtained from XRD studies on **2a** support thiolate coordination. Analysis of single crystals that diffracted to 1.70 Å resolution revealed formation of a mononuclear Cu complex within each subunit in which the Cu center has an N_3S primary coordination sphere (Figure S4B). The dpea ligand adopts a facial orientation around the immobilized Cu center in **2a** producing an average Cu–N bond distance of 2.10(2) Å and a Cu–S1 bond length of 2.18(2) Å (Table 2). The Cu^{II} complex has N1-Cu-N2, S1-Cu-N1, and S1-Cu-N2 bond angles of 92(3)°, 129(2)°, and 113(2)° that forms a distorted trigonal plane with the Cu positioned 0.62 Å from the plane. In addition, a relatively long N2-Cu-N3 bond angle of 127(2)° was observed.

More intense bands at λ_{max} ~ 600 nm were obtained for **2b** and **2c** and the higher energy bands at λ_{max} ~ 445 nm were weaker in intensity compared to **2a** (Figure 2, Table 1).

These new optical data produce *Re* values of 0.29 for **2b** and 0.44 for **2c** both of which are significantly lower than that in **2a** and are approaching values that normally are associated with classical blue copper sites. Structural studies on **2b** support that the Cu centers in these ArMs are distinct from that in **2a** and more comparable to classical Type I Cu sites. The molecular structure of **2b** from XRD data collected to 1.70 Å resolution, again, revealed a mononuclear, 4-coordinate Cu complex with an N_3S primary coordination sphere (Figure 3A). However, noticeable differences were observed in the structure of the Cu complex in **2b** compared to those in **2a**. The Cu center in **2b** is positioned 1.3 Å further from the biotin binding site, an adjustment that places the pyridine ring containing N2 nearer to residue L124 and that places N3 nearer to residue T114 (Figure 3C). To avoid steric clashing, a significant contraction of the N2-Cu-N3 angle results from 127° in **2a** to 96° in **2b** (Table 2). These changes in structure for **2b** result in an immobilized trigonal monopyramidal Cu complex that has similar properties to Type I Cu centers. For instance, the N1-Cu-N2, S1-Cu-N1, and S1-Cu-N2 bond angles of 92(3)°, 124(2)°, and 132(2)° are nearly equivalent to the related angles found in the azurin $M_{121}H$[32] and stellacyanin (Table 2).[30] In addition, the Cu–S1 bond length in **2b** has contracted to 2.11(2) Å and the Cu center is displaced only 0.41 Å from the trigonal plane, which is closer to those found in Type 1 Cu sites (Table 2). We have also solved the molecular structure of **2c** to 1.40 Å resolution and the structure of the Cu complex is similar, but not identical to **2b,** (Table 2, Figure S4D) with the Cu center moving 0.82 Å further from the biotin binding site.

The properties of **2a-c** determined from S- and X-band EPR spectroscopy exhibited considerable differences in comparison to ArMs with Sav WT as the host (**1a-c**).[33,34] New methods we introduce here use the spectra from two microwave frequencies, paired with simulation, to determine the A-tensors in the absence of resolved hyperfine splittings. The EPR spectra for **2a** showed a 4-line hyperfine pattern at $g_z = 2.19$ with a reduced A_z value of 353 MHz compared to the average A_z value of 523 MHz obtained for **1a**. The lowering of the A_z-value in **2a** is consistent with Cu-S_{cys} interaction in the ArM. The EPR spectra for **2b** and **2c** are dramatically different from that of **2a**. Normally for Cu(II) complexes, the large hyperfine splitting for $A_z = A_{\|}$ is associated with $g_z = g_{\|}$. This is not the case for **2b** and **2c**, in which the g_z-values of 2.18 and 2.19 have associated A_z-values that are low (71 or 79 MHz, respectively). The largest hyperfine splitting values were found in the perpendicular direction: A_y–values of 264 (**2b**) and 225 MHz (**2c**) were determined from our simulations with A_x-values closer to zero (Table 1). These values indicate a rhombic A-tensor that deviates significantly from axial symmetry, in contrast to the g-tensor that is nearly axial. The combination of low A_z-values and rhombic A-tensors for **2b** and **2c** is rare and is directly linked to their protein-induced coordination spheres. The small A_z-value for **2b** and **2c** is indicative of relatively large covalency that is consistent with the short Cu–S_{cys} bond lengths observed in the XRD studies.[20] The rhombic A-tensor indicates a significant admixture of the d_z^2 orbital into the singly occupied d_x^2-y^2. Our findings for **2b** and **2c** are similar to those reported for stellacyanin and the $M_{121}H$ variant of azurin (Table 1).[28]

The redox properties of the Cu ArMs were measured using cyclic voltammetry (Figure S6): **1a** contains a reversible one-electron process for the Cu(II)/(I) couple at $E_{1/2} = 70$ mV versus NHE that shifts to 140 mV in **2a**. This positive shift for the $S_{112}C$ variant is expected

for a thiolate-ligated Cu center, and the potential of 140 mV approaches those reported for Type I proteins. The CVs of **1b-c** and **2b-c** are less reversible than **1a** and **2a** but exhibit a similar trend with an increase in E_a of ~70 mV for **2b** versus **1b** and ~35 mV for **2c** versus **1c** (Figure S7). This shift to positive potentials most likely reflects a more covalent Cu–S_{cys} bond in **2b2c**.

The results for our artificial Cu proteins revealed important design features for using Sav to confine coordination complexes. ArMs with Sav WT produced Cu complexes having nearly identical properties that are similar to those found in synthetic Cu species. However, the $S_{112}C$ variant of Sav produced artificial Cu proteins **2a-c** that have markedly different properties caused by the presence of an endogenous thiolate ligand. Moreover, we were able to tune the position of the Cu centers within Sav $S_{112}C$ by varying the linker between the biotin and the metal complex that produced commensurate changes in the properties of the Cu complexes. This method was ineffective with Sav WT in which the the linker length had little effect on the confined species, suggesting that one-point binding through the biotin-Sav interaction may not be enough to regulate the placement of a metal complex within Sav. Coupling the ability to vary the linker with additional anchoring via endogenous ligand coordination offers a versatile means to fine-tune the properties of the metal cofactors.

The properties of **2b** and **2c** also illustrate the potential of this approach to model active sites of metalloproteins. The ability to modify the Sav host to engineer endogenous ligands, combined with synthetic ligands, produces new types of coordination spheres around the immobilized Cu centers that cannot be readily accessed in a pure synthetic construct. The formation of stable complexes with discrete Cu-S_{cys} bonds in **2a-c** was achieved by taking advantage of a Sav variant as the protein host. These results further highlight the benefits of this approach in modulating the structure and properties of an immobilized metal complex to obtain new structures.

Supplementary Material

Refer to Web version on PubMed Central for supplementary material.

ACKNOWLEDGMENT

The authors thank the NIH (GM50781-21S1 to ASB and TRW and GM77387 to MPH) for financial support. We thank T. Poulos, H. Li and J. Klehr for assistance.

REFERENCES

1. Cook SA, Borovik AS. Acc. Chem. Res. 2015; 48:2407. [PubMed: 26181849]
2. Shook RL, Borovik AS. Inorg. Chem. 2010; 49:3646. [PubMed: 20380466]
3. Liu J, Chakraborty S, Hosseinzadeh P, Yu Y, Tian S, Petrik I, Bhagi A, Lu Y. Chem. Rev. 2014; 114:4366. [PubMed: 24758379]
4. DeGrado WF, Summa CM, Pavone V, Nastri F, Lombardi A. Annu. Rev. Biochem. 1999; 68:779. [PubMed: 10872466]
5. Bos J, Browne WR, Driessen A, Roelfes G. J. Am. Chem. Soc. 2015; 137:9796. [PubMed: 26214343]
6. Delapierre CM, Rondot L, Cavazza C, Ménage S. Israel J. Chem. 2015; 55:61.

7. Song WJ, Tezcan FA. Science. 2014; 346:1525. [PubMed: 25525249]
8. Berggren G, Adamska A, Lambertz C, Simmons TR, Esselborn J, Atta M, Gambarelli S, Mouesca JM, Reijerse E, Lubitz W, Happe T, Artero V, Fontecave M. Nature. 2013; 499:66. [PubMed: 23803769]
9. Hosseinzadeh P, Marshall NM, Chacón KN, Yu Y, Nilges MJ, New SY, Tashkov SA, Blackburn NJ, Lu Y. Proc. Natl. Acad. Sci. USA. 2016; 113:262. [PubMed: 26631748]
10. Weber PC, Ohlendorf DH, Wendoloski JJ, Salemme FR. Science. 1989; 243:85. [PubMed: 2911722]
11. Wilson ME, Whitesides GM. J. Am. Chem. Soc. 1978; 100:306.
12. Dürrenberger M, Ward TR. Curr. Opin. Chem. Biol. 2014; 19:99. [PubMed: 24608081]
13. Solomon EI, Hadt RG. Coord. Chem. Rev. 2011; 255:774.
14. LaCroix LB, Randall DW, Nersissian AM, Hoitink CWG, Canters GW, Valentine JS, Solomon EI. J. Am. Chem. Soc. 1998; 120:9621.
15. Olesen K, Veselov A, Zhao Y, Wang Y, Danner B, Scholes CP, Shapleigh JP. Biochemistry. 1998; 37:6086. [PubMed: 9558347]
16. Daugherty RG, Wasowicz T, Gibney BR, DeRose VJ. Inorg. Chem. 2002; 41:2623. [PubMed: 12005485]
17. Plegaria JS, Duca M, Tard C, Friedlander TJ, Deb A, Penner-Hahn JE, Pecoraro VL. Inorg. Chem. 2015; 54:9470. [PubMed: 26381361]
18. Kitajima N, Fujisawa K, Tanaka M, Moro-oka Y. J. Am. Chem. Soc. 1992; 114:9232.
19. Holland PL, Tolman WB. J. Am. Chem. Soc. 1999; 121:7270.
20. Randall DW, George S, Hedman B, Hodgson KO, Fujisawa K, Solomon EI. J. Am. Chem. Soc. 2000; 122:11620.
21. Karlin KD, Kaderli S, Zuberbühler AD. Acc. Chem. Res. 1997; 30:139–147.
22. Skander M, Humbert N, Collot J, Gradinaru J, Klein G, Loosli A, Sauser J, Zocchi A, Gilardoni F, Ward TR. J. Am. Chem. Soc. 2004; 126:14411. [PubMed: 15521760]
23. Crystals of 1b and 1c did not provide suitable data.
24. Thyagarajan S, Murthy NN, Sarjeant AAN, Karlin KD, Rokita SE. J. Am. Chem. Soc. 2006; 128:7003. [PubMed: 16719480]
25. Zimbron JM, Heinisch T, Schmid M, Hamels D, Nogueira ES, Schirmer T, Ward TR. J. Am. Chem. Soc. 2013; 135:5384. [PubMed: 23496309]
26. Malmström BG, Reinhammar B, Vänngård T. Biochim. Biophys. Acta. 1970; 205:48. [PubMed: 4314765]
27. Reinhammar BR. Biochim. Biophys. Acta. 1972; 275:245. [PubMed: 4342730]
28. Kroes SJ, Hoitink CW, Andrew CR, Ai J, Sanders-Loehr J, Messerschmidt A, Hagen WR, Canters GW. Eur. J. Biochem. 1996; 240:342. [PubMed: 8841397]
29. Hosseinzadeh P, Tian S, Marshall NM, Hemp J, Mullen T, Nilges MJ, Gao Y-G, Robinson H, Stahl DA, Gennis RB, Lu Y. J. Am. Chem. Soc. 2016; 138:6324. [PubMed: 27120678]
30. Hart PJ, Nersissian AM, Herrmann RG, Nalbandyan RM, Valentine JS, Eisenberg D. Protein Sci. 1996; 5:2175. [PubMed: 8931136]
31. Messerschmidt A, Prade L, Kroes SJ, Sanders-Loehr J, Huber R, Canters GW. Proc. Natl. Acad. Sci. USA. 1998; 95:3443. [PubMed: 9520385]
32. Baker EN. J. Mol. Biol. 1988; 203:1071. [PubMed: 3210236]
33. Lancaster KM, Zaballa M-E, Sproules S, Sundararajan M, DeBeer S, Richards JH, Vila AJ, Neese F, Gray HB. J. Am. Chem. Soc. 2012; 134:8241. [PubMed: 22563915]
34. All EPR spectra of the Cu ArMs with $S_{112}C$ contained varying amounts (20 to 50%) species with features the same as those found in 1a-1c that were subtracted from the spectra in Figure 4. Complete details are found in the supporting information.

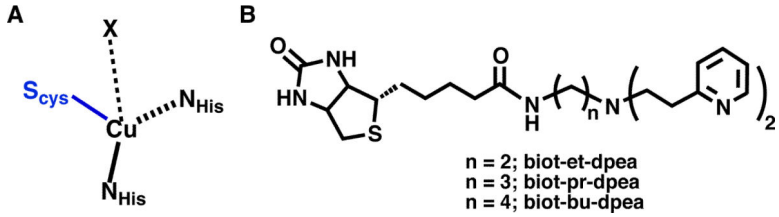

Figure 1.

Primary coordination sphere of Type 1 Cu center (**A**) and biotinylated ligands used in this study (**B**).

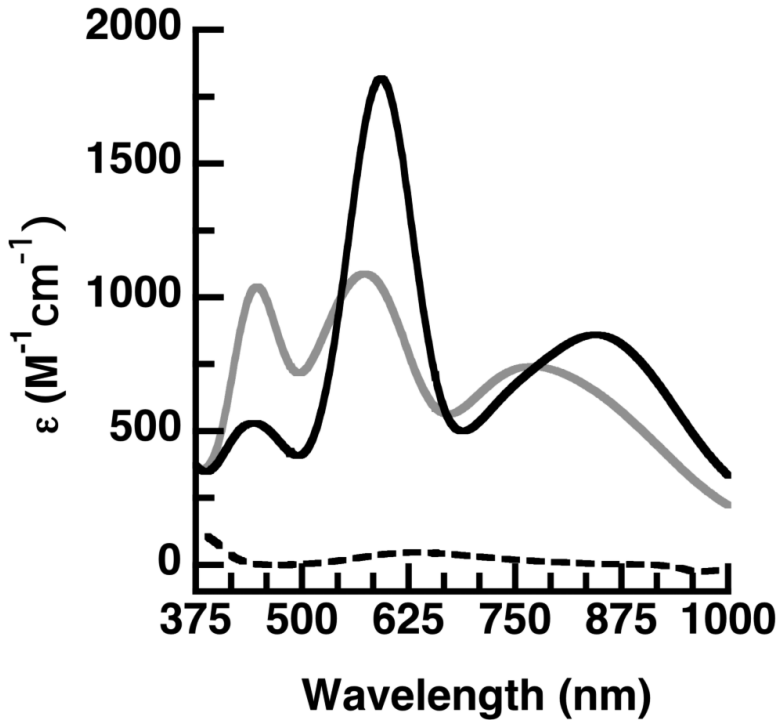

Figure 2.
Absorbance spectra for **1a** (---), **2a** (gray), and **2b** (black).

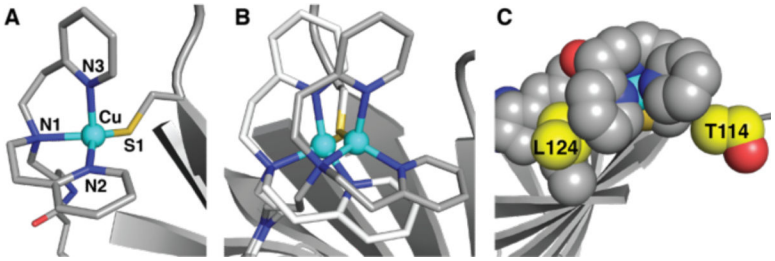

Figure 3.

Structure of **2b** (**A**), structural overlay of **2a** (white) and **2b** (gray) (**B**), and space-filling representation of **2b** highlighting interactions with residues (yellow) of the protein host (**C**).

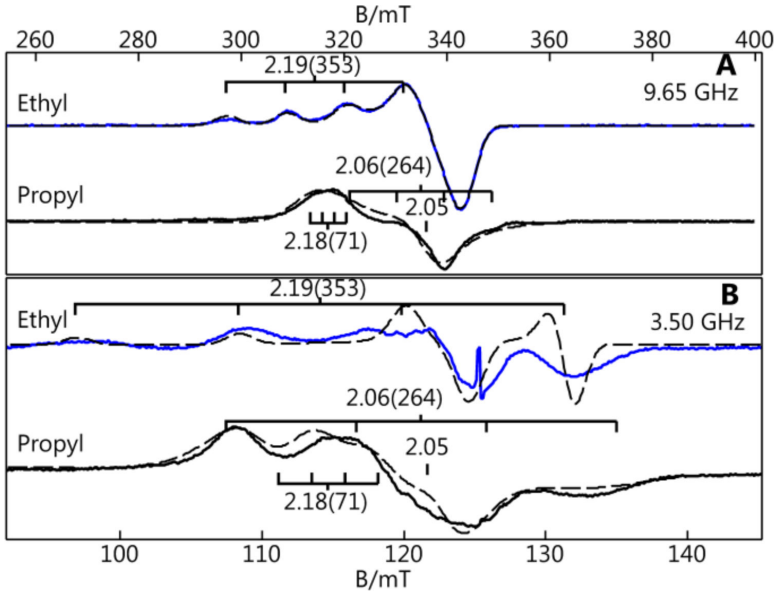

Figure 4.

X- (**A**) and S-band (**B**) difference EPR spectra for **2a** (blue) and **2b** (black). Simulations are dashed lined. Minor amounts of WT ArMs were subtracted from each spectrum.[28] The g-values and (A-values in MHz) as indicated.

Table 1

Properties for 2a-c and selected cupredoxins.

Host	S112C			Stellacyanin[a]	Azurin
n	et (2a)	pr (2b)	bu (2c)		$M_{121}H$[b,c]
λ_{max},nm (ε_M)	448 (1040)	443 (530)	437 (780)	440 (1090)	439 (NR)
	574 (1090)	593 (1820)	611 (1790)	595 (4970)	593 (NR)
	771 (740)	846 (860)	891 (840)	781(690)	
				893(580)	
Re	0.95	0.29	0.44	0.22	1.8
g	2.02	2.05	2.06	2.02, 2.08	2.05
	2.07	2.06	2.08		2.05
	2.19	2.18	2.19	2.29	2.25
A, MHz	nd, nd, 353	17	4	171	27, 27, 305
		264	225	87	
		71	79	105	
$E_{1/2}$ mV[d]	140	110	95	184	<200

[a] refs. 14,26,27

[b] ref. 28

[c] pH=6

[d] NHE, rt, 50 mM MES pH 6

Table 2

Selected Bond Lengths (Å) and Angles (°) for 2a-c, Stellacyanin, and $M_{121}H$ Azurin.

Host	$S_{112}C$			Stellacyanin[b]	Azurin,[c,d]
n	et (2a)	pr (2b)	bu (2c)		$M_{121}H$
Cu-N1	2.19(2)	2.24(2)	2.28(2)	2.04(2)	2.02(1)
Cu-N2	2.03(2)	2.05(2)	2.10(2)	1.96(2)	2.06(1)
Cu-N3	2.09(2)	2.20(2)	2.12(2)	–	2.24(1)
Cu-S1	2.18(2)	2.11(2)	2.09(2)	2.18(2)	2.25(1)
$d[Cu\text{-}(N/S)_t]$[a]	0.62	0.41	0.66	0.32	0.58
N1-Cu-N2	92(3)	92(3)	89(3)	101(3)	98(3)
N1-Cu-S1	129(3)	124(3)	124(3)	118(3)	109(3)
N2-Cu-S1	113(3)	132(3)	118(3)	134(3)	130(3)
N1-Cu-N3	97(3)	94(3)	87(3)	–	126(3)
N2-Cu-N3	127(3)	96(3)	105(3)	–	89(3)
N3-Cu-S1	100(3)	110(3)	124(3)	–	106(3)

[a] Distance of Cu from trigonal plane

[b] ref. 30

[c] ref. 31

[d] pH 6